Hybrid CNN assisted Computer Aided Diagnosis System for Glaucoma Detection and Classification: GlaucoNet+

Naganagouda Patil, P V Rao, Preethi N Patil

Abstract—The exponential rise in technologies has revitalized academia-industries to achieve more efficient computer aided diagnosis systems. It becomes inevitable especially for Glaucoma detection which has been increasing with vast pace globally. Most of the existing approaches employs morphological features like optical disk and optical cup information, optical cup to disk ratio etc; however enabling optimal detection of such traits has always been challenge for researchers. On the other hand, in the last few years deep learning methods have gained widespread attention due to its ability to exploit fine grained features of images to make optimal classification decision. However, reliance of such methods predominantly depends on the presence of deep features demanding suitable feature extraction method. To achieve it major existing approaches extracts full-image features that with high dimensional kernel generates gigantically huge features, making classification computationally overburdened. Therefore, retaining optimal balance between deep features and computational overhead is of utmost significance for glaucoma detection and classification. With this motive, in this paper a novel hybrid deep learning model has been developed for Glaucoma detection and classification. The proposed Hybrid CNN model embodies Stacked Auto-Encoder (SAE) with transferable learning model AlexNet that extracts high dimensional features to make further two-class classification. To achieve computational efficiency, In addition to the classical ReLu and dropout (50%), we used Principle Component Analysis (PCA) and Linear Discriminant Analysis (LDA) algorithms. We applied 10-fold cross validation assisted Support Vector Machine classifier to perform two-class classification; Glaucomatous and Normal fundus images. Simulation results affirmed that the proposed Hybrid deep learning model with LDA feature selection and SVM-Poly classification achieves the maximum accuracy of 98.8%, precision 97.5%, recall 97.5% and F-Measure of 97.8%.

Keywords: Glaucoma detection, Deep Learning, Transferable Convolutional Neural Network, GaluocNet+, Computer Aided Diagnosis System.

I. INTRODUCTION

The high pace rise in software computing technologies, vision technologies and hardware has benefitted different socio-economic stakeholders by facilitating time as well as cost-efficient decision making purposes. Amongst the major purposes, it has gained wide-spread attention to serve healthcare demands for efficient and productive CAD solutions. In the last few years Glaucoma disease has surfaced as one of the most causative factors damaging human vision [1]. Glaucoma is a type of irreversible eye-disorder that damages optic nerve and degrades vision capacity [1]. In fact, it has been identified as the most causative factor for blindness, which might reach around 20 million people by or before 2020 [1]. Typically, it remains undetected for long time and therefore remains undetected in its early stages [3]. Due to such reason, it is also called as the "silent theft of sight". In major Glaucoma cases, a person doesn't feel any pain or symptoms and therefore its detection becomes possible only when it reaches to the advanced stage. Glaucoma being an irreversible eye-disease affects the optical nerve which is responsible for accommodating information from the eye to the brain causes blindness and ocular hypertension [2]. In general, there are three dominant methods practiced for Glaucoma detection [4]; Intraocular Pressure (IOP) measurement, Function-Based Visual Field Test (FBVFT), and Optic Nerve Head (ONH). Though, IOP states a significant risk factor it can't be universally robust to detect Glaucoma for different stages with varied clinical-measurement values [4]. Similarly, FBVFT requires specific peri-metric and sophisticated tools which are costly and commonly not available in major primary healthcare centers. ONH examination is an expedient paradigm to identify Glaucoma in its early stage, and is contemporarily performed by professional and skilled Glaucoma specialists [5-7]. However, it is time consuming, costly and sometime inaccurate [7]. Functionally, it employs varied morphological parameters like Vertical Cup to Disc Ratio (CDR) [8], Rim to Disc Area Ratio (RDR), NRR, and Disc Diameter [9] to detect Glaucoma in the retinal fundus images. CDR methods have been extensively used where a larger CDR signifies higher Glaucoma-risk [4]. Noticeably, these clinical parameters are the region of interest which are assessed to signify any presence of Glaucomatic feature in retinal fundus images. Functionally, a CAD solution for automatic Glaucoma detection comprises ROI detection, segmentation, features extraction and classification [10]. To detect Glaucoma it employs measurement-based approach [10-14], where at first it localizes ROI and extracts allied features (clinical measurement values). To achieve optimal CAD solution for Glaucoma detection accurate ROI segmentation is must. To achieve it, different methods like super-pixel based classifier in conjunction with the different visual features like OD, OC and CDR etc have been applied [12][15]. However, maintaining optimal accuracy under different spatio-temporal features of the human eye is difficult. Complexities like the presence of nerves over the

Revised Manuscript Received on October 15, 2019.

Naganagouda Patil, Research Scholar, Department of ECE, T John Institute of Technology, Bangalore -560083 and Affiliated to Visvesvaraya Technological University,Belagavi,Karnataka, India (Email: ncpatil@gmail.com)

P V Rao, Research supervisor, Department of ECE, T John Institute of Technology, Bangalore, VBIT, Hyderabad, T,S., India-501301 (Email: raopachara@gmail.com)

Preethi N Patil Asst Professor, Dept Of MCA, R V College of Engineering Bangalore-560059(preethinpatil@rvce.edu.in)

disk surfaces make segmentation difficult. Though, above stated clinical measurements have been used extensively for Glaucoma detection, the processes like pre-processing, segmentation, post-segmentation, the presence of morphological differences and nerves over OD etc make it computationally complex.

In last few years, Deep Learning (DL) technique has emerged as a potential approach to perform target detection and classification without imposing computational overheads. Considering Glaucoma detection as purpose, authors [14] applied a multi-label DL concept to segment OD and OC region based on which CDR was obtained to be used for verification. Learning-based methods with learned classifiers have performed better by exploiting different visual features from the fundus image to assist automatic Glaucoma detection and classification [16-20]. In comparison to the classical clinical measurements, deep learning methods extracts extracted visual features that provides more goal-centric information to make optimal decision [4]. In fact, DL methods have exhibited better performance to generate significant and highly discriminative representations for varied computer vision based applications [20], including CAD and medical image analysis [21-23]. Convolutional Neural Networks (CNNs) possess robust learning ability due to its scaling, shifting, translation, manipulation and rotation of the inputs with extreme diversity and non-linearity. In addition, it is designed specifically to analyse and classify visual patterns directly from pixel images without imposing pre-processing and segmentation tasks. CNNs have been examined for it efficacy for retinal vessel detection [4][24][25], Glaucoma detection [26][27], etc. Though, a few DL methods have been developed for Glaucoma detection and classification, majority of the works either employed clinical measurements as feature for classification or conventional CNN models. However, the questions whether the extracted features were sufficient to make self-sufficient and automatic Glaucoma detection and classification remained a question. The classical CNN models apply low dimensional features to perform detection; on contrary literature reveal that the high dimensional features can provide more accurate and reliable performance. However, extracting deep features require more computational efficiency. Thus, maintaining an optimal balance between deep features and computational efficiency can enable a robust and efficient solution for Glaucoma detection and classification. Considering it as motivation, in this paper the focus is made on developing a novel and robust Hybrid deep learning model by employing Stacked Auto Encoder (SAE) and transferable CNN model named AlexNet. Once performing standard pre-processing functions over the input fundus images, we have executed the proposed dual phase feature extraction method where at first SAE extracts the key features, which is followed by AlexNet based feature extraction. Thus, obtaining the both deep learning features, it has been fused to yield a single feature set, which is later processed for feature selection using Principle Component Analysis (PCA) and Linear Discriminant Analysis (LDA). Noticeably, the prime objective of applying PCA and LDA is select only significant features by reducing redundant or low-significant features so as to achieve computational efficiency. Obtaining the optimal feature set, our proposed method applies SVM with 10-fold cross validation to perform two-class classification (i.e., Glaucoma or Non-Glaucoma). The overall proposed system has been implemented using MATLAB 2018a. To assess performance confusion metrics has been obtained that retrieves performance in terms of accuracy, precision, recall, and F-Measure. The performance comparison reveals that the proposed method outperforms existing approaches while assuring optimal trade-off between performance and computational overheads.

The remaining sections of the presented manuscript are divided as follows: Section II discusses the related work, which is followed by research questions in Section III. Section IV discusses the problem formulation and implementation in Section IV. The results obtained are discussed in Section V. Overall research conclusion and future scopes are discussed in Section VI. References used are mentioned at the end of the manuscript.

II. RELATED WORK

Authors [28] designed a hierarchical method by using clustering, morphological traits identification to perform Glaucomatous visual field defect patterns identification. Authors [29] designed Retina Nerve Fiber Layer Defect (RNFLD) detection model by applying patch features driven recurrent neural network (RNN). In [30] authors focused on detecting the RNFL thickness using Optical Coherence Tomography (OCT) images for glaucoma detection. With goal to reduce static threshold based detection complexities and limitation, authors [31] proposed adaptive threshold based blood vessel detection model where they applied Gabor filter and Top-Hat transform [32] for feature extraction, followed by Extreme Learning Machine (ELM) algorithm for classification. Realizing the need of multiple-feature sets, authors [33] applied both structural as well as textural features; Structural Features (HSF) and Hybrid Textural Features (HTF). They applied SVM as machine learning classifier for two-class classification. Spatiotemporal features like OD, OC and its curve variations were used in [34] for glaucoma prediction. Authors [34] applied Hough transformation to extract features of the detected OD. Realizing the fact that the spatio-temporal features of human eye can vary, authors [35] exploited multiple morphological features including CDR [37], Horizontal to Vertical CDR (H-V CDR), Cup to Disc Area Ratio (CDAR), and Rim to Disc Area Ratio (RDAR) and Neuro-Retinal Rim (NRR) to perform Glaucoma detection. In major CDR based approaches, authors didn't consider segmentation error that could have decisive impact on accuracy. To alleviate it, authors [38] introduced Polar transform based unsupervised algorithm for automatic OC segmentation. Obtaining morphological features (i.e., CDR and NRR), authors [39] used watershed transformation algorithm to detect Glaucoma. They used adaptive threshold based method for CDR and NRR segmentation. The extracted features from the CDR and NRR were used as input for SVM based two-class classification. Authors [40]

used CDR features obtained through super-pixels clustering algorithm, simple linear iterative clustering (SLIC) and a feed-forward neural network classifier to perform two-class classification. To reduce computational overheads, authors [41] extracted only a part of the eye sclera and estimated its percentage to perform Glaucoma detection. However, its performance can't be generalized as the aforesaid trait might vary over one to another person. Authors [42][43] developed a self assessed OC and OD segmentation scheme to further derive CDR for static threshold based glaucoma detection. However, applying static threshold for classification and generalization seems biased [56]. Once, obtaining features authors [42] applied edge detection method with GVF Snake Active Contour for Glaucoma detection. Unfortunately, majority of the classical CDR methods show inaccurate performance, especially during cup detection over the horizontally identified disk region [44-47][48-50]. Authors [51] focused on applying adaptive threshold based methods and green channel extraction concepts to perform Glaucoma detection and classification. In [52], authors used active contour propagation based blood vessel segmentation to enhance CDR estimation accuracy [52][53]. In [54], authors estimated OD center using thresholding and distance transformation technique, which was then followed by the estimation of Eigenvector spaces of normal set and glaucoma using PCA algorithm. As classifier, authors [54] applied different algorithms like Bayes classifiers [54], K-NN [50], logistic regression [55]. Authors [55] applied GLCM with linear transformation technique to perform Glaucoma detection.

In [57] too Haralick Texture Features were obtained from the digital fundus images which were later classified using K Nearest Neighbor (KNN) algorithm for Glaucoma detection and classification. Authors in [58] emphasized on minimizing the segmentation complexity. To achieve it, they recommended deep learning methods with ability to exploit image-relevant information to make Glaucoma classification. In [59] multi-model network known as G-EyeNet was developed that comprised a deep convolutional auto-encoder (CAE) to perform Glaucoma detection. Authors [60] applied CNN for automatic Glaucoma detection and found it suitable for target detection purposes [61] [62]. To enhance accuracy cross-validation concept was suggested in [63].

III. RESEARCH QUESTIONS

The overall research intends to find out the optimal answers for the following:

RQ1: *Can the use of CNN be a potential and reliable solution for Glaucoma detection and classification?*

RQ1: *Can SAE extracted features with a transferable CNN model like AlexNet be a robust architecture for deep-feature extraction and classification?*

RQ1: *Can the use of high dimensional features be significant to perform Glaucoma detection and classification?*

RQ1: *Unlike conventional dropout based method, can the use of PCA and LDA algorithms be effective to retain significant deep features for glaucoma detection and classification?*

RQ1: *Can the use of N-fold cross validation with SVM be efficient for glaucoma detection and classification?*

IV. PROBLEM FORMULATION

Although, CNN methods have gained wide-spread attention for image analysis and classification purposes, however retaining maximum possible deep features and maintaining optimal computational efficiency has always been the challenge. On the other hand, only applying morphological or clinical measurement as decision parameters can't guarantee accuracy of the Glaucoma detection. Considering these facts, designing a robust and computationally efficient deep learning model by inheriting deep features to be processed under enhanced learning environment can achieve better CAD solution towards Glaucoma diagnosis. Considering it as motive, in this paper a multi-phased optimization concept it developed which exploits efficiency of enhanced pre-processing, SAE-CNN and a transferable deep learning concept (AlexNet) to extract most significant and deep features from fundus images for Glaucoma detection and classification. Realizing the fact that the inclusion of two deep learning models and allied features, especially 4096 dimensional AlexNet features, in this research different feature selection methods have been applied that retains only the vital features to make optimal classification. Noticeably, the extraction methods, SAE CNN and AlexNet CNN are applied in parallel that obtains features distinctly. Noticeably, SAE-CNN extracts low dimensional features (256 kernels), while AlexNet CNN extracts high dimensional features at FC6 and FC7, i.e., 4096 dimensional features to perform glaucoma detection and classification. The features extracted by Convolutional Stacked Auto-Encoder and (SAE) AlexNet CNN are concatenated together to obtain a cumulative feature vectors which is projected as input to the SVM for two-class classification. Observing above stated feature extraction method, it can be found that the dual phased features extraction might impose significantly huge computational overheads and give rise to large feature set. To alleviate such computational overheads in this paper we have implemented PCA and LDA based feature selection and/or dimensional reduction methods that retain only significant features to perform two-class classification. As a classification system, in this paper we have applied SVM with 10-fold cross validation. Considering non-linearity of the feature patterns we have applied SVM with different (linear, polynomial and radial basis function) kernel functions for two-class classification. Considering diversity of data and real-time relevance we have considered DRISHTI-GS and DRION-DB fundus datasets.

The detailed discussion of the proposed GlaucoNet+ model is given in the sub-sequent sections.

V. SYSTEM MODEL

The overall proposed system has been accomplished in the following phases (Fig. 1).

1. *Data Acquisition and Preparation,*
2. *Preprocessing,*
3. *Dual-Phased SAE CNN and AlexNet CNN assisted*

Feature Extraction and learning,

4. *PCA/LDA based Feature Selection, and*
5. *Two-class classification using SVM with N-Fold Cross validation.*

A. Datasets Acquisition and Preparation

Realizing the fact that the different benchmark datasets (i.e., fundus images) used to have the different spatio-temporal features and therefore assessment of the proposed model with the different benchmarks (dataset) can give better performance visualization. With this motive, in this research work two different fundus image datasets named DRISHTI-GS and DRION-DB have been considered. DRISHTI-GS fundus datasets comprises a total of 100 fundus images having different spatio-temporal features. Similarly, DRION-DB dataset comprised 110 fundus images. Undeniably, the considered fundus images were having different spatio-temporal constructs such as lighting conditions, OD and OC position, morphological conditions, nerve presence etc. The considered datasets comprised images of both types, fundus images with glaucoma and without glaucoma or normal fundus images. As standard pro-processing, the input images were at first converted into RGB to gray which was processed further for image resizing which was done for the 256×256 dimension before performing feature extraction.

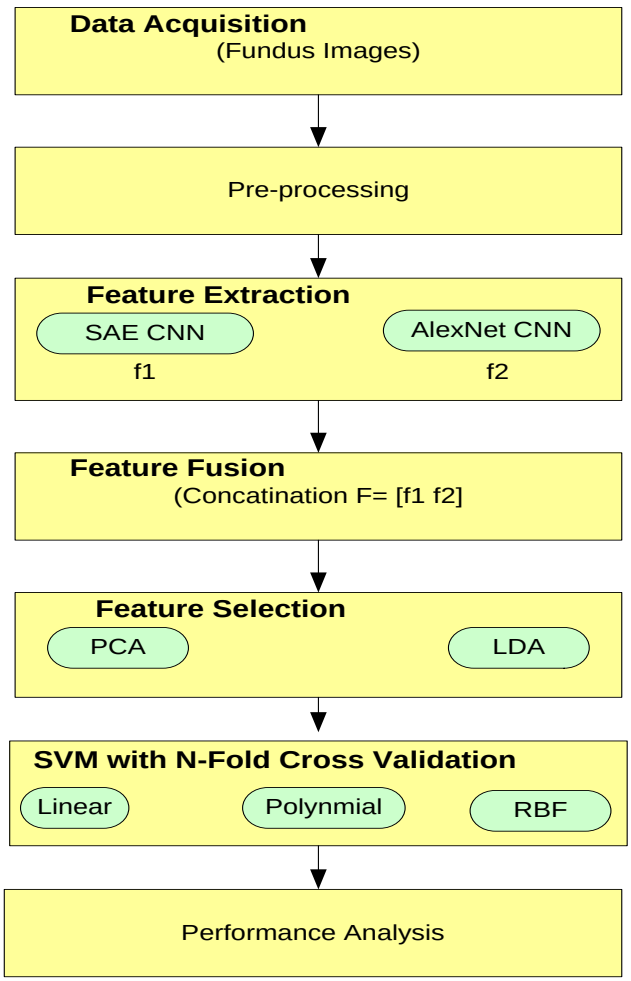

Fig 1 GlaucoNet+ implementation

Table I presents a snippet of the Glaucoma fundus datasets used in this research.

B. Preprocessing

Undeniably, the quality of data has a greater impact on the classification accuracy and efficiency. To ensure that the data is suitable for processing, the pre-processing technique is performed. In this system the preprocessing model helps in obtaining precise nuclei and achieves better identification and characterization. In Glaucoma detection the glaucoma size should be identified carefully. The pre-processing technique ensures that the suppression of the original image is needed to identify important texture and other features. In this model the pre-processing approach is done before executing feature extraction. During the pre-processing of images the RGB images are converted into grey color, followed by intensity equalization that alleviates the issues caused due to different illuminations and lighting conditions. To retain optima computational efficacy the input fundus images were resized to 256×256 dimensions. Once performing pre-processing the processed images were fed as input to the proposed dual phased feature extraction model, where two distinct algorithms Stacked Convolutional Auto-Encoders and AlexNet CNN were applied individually to perform feature extraction.

Table I Samples of the different Fundus images

DRION-DB	DRISHTI-GS
	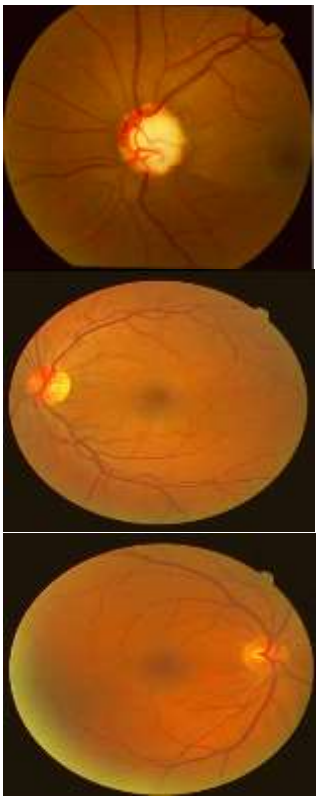

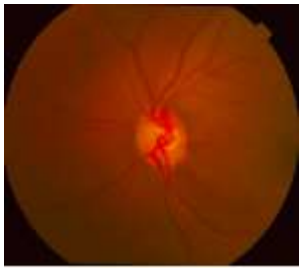


***These are some of the samples fundus images pertaining to DRION-DB and DRISHTI-GS datasets**

C. Dual-Phased SAE and AlexNet CNN assisted Feature Extraction and learning

In this phase we have applied dual phased feature extraction, where at first Auto-Encoder assisted CNN model has been applied that extract deep features which is then projected as input to AlexNet CNN that extracts high dimensional features to be further classified. The approaches applied are:

1. Stacked Auto-Encoder (SAE) based feature extraction, and

2. AlexNet CNN based high dimensional feature extraction.

The detailed discussion of the proposed feature extraction model is given in the sub-sequent sections.

a). Stacked Auto-Encoder based Feature Extraction

This section briefs a snippet of Auto-Encoder CNN based feature extraction. Before discussing Auto-Encoder CNN a brief of Auto-Encoder is given as follows:

Auto-Encoders signify a kind of unsupervised learning approach that uses an input $x \in R^d$ to map it to obtain the latent representation$h \in R^{d'}$. In general, it is accomplished by using deterministic function $h = f_\theta = \sigma(W_x + b)$ that in conjunction with functions $\theta = \{W, b\}$ with W as the weight and $b$as the bias values. In the subsequent phase, Auto-Encoder performs reverse mapping of the function f to reconstruct the input and retrieves the reconstructed feature$y = f_{\theta'}(h) = \sigma(W'h + b')$. To perform encoding of the input, and respective decoding (of the mapped latent representation of the encoded data), the two parameters are conditioned to satisfy $W' = W^T$ by using same weights. The input patterns, say training patterns x_i are mapped distinctly onto its code h_i that gives rise to the reconstruction y_i, while the parameters are optimized by minimizing a cost function over the training set $D_n = \{(x_0, t_0), \dots, (x_n, t_n)\}$. Our proposed Auto-Encoder learns the identity mapping without using any additional constraints. To achieve better accuracy over non-linear mapping patterns we have applied de-noising auto-encoders (DAs) that reconstructs optimal input fundus image data even under spatio-temporal noise and data corruption conditions. Let $\bar{x}$ be the corrupted or noised data of the input x. Our proposed Auto-Encoder is executed to de-noise the inputs by estimating the latent representation $h = f_{\theta'}(\bar{x}) = \sigma(W\bar{x} + b)$ that eventually helps retrieving original image or reconstructed image$y = f_{\theta'}(h) = \sigma(W'h + b')$. In our proposed method DA forms a hierarchical learning scheme. The proposed approach behaves as a Hierarchical Feature Extractor (HFE) that scales input fundus images to the high-dimensional features for further processing. Our proposed Auto-Encoder model learns non-trivial features using Scale Conjugate Gradient Algorithm (SCGA) to obtain significant CNN initialization. It helps avoiding key problem like Local Minima (LM), which is a common issue in major Deep Learning (DL) models. To achieve better performance, the extracted feature from Auto-Encoder has been relearned by means of SAE architecture. Noticeably, we have applied SAE model to obtain more efficient features so as to achieve potential deep features for further classification. In our proposed SAE model, we have applied multiple Auto-Encoders stacked in a cascaded manner that eventually constitutes a deep hierarchy, where each (ascending) layer retrieves its input from the latent representation of its descending (below) layer. In our proposed SAE model output of each layer is connected to the input layer or other, where the sparsity feature has been incorporated to reduce the reconstruction error swiftly. In addition, the use of sparcity features achieves higher accuracy.

A brief of our proposed SAE feature extraction model and its implementation is given as follows:

SAE comprises n layers (we used n=2) possessing weight parameters $\mathrm{W}^{(\mathrm{k},1)}$, $\mathrm{W}^{(\mathrm{k},2)}$, and respective bias values $\mathrm{b}^{(\mathrm{k},1)}$and $\mathrm{b}^{(\mathrm{k},2)}$. Noticeably, $\mathrm{b}^{(\mathrm{k},\mathrm{n})}$ signifies bias values for the k-th Auto-Encoder. Functionally, Auto-Encoder employs two functions, encoding and decoding where the encoding part of the each layer in the forward order is stated as (1-2).

$$a^{(l)} = f\left(z^{(l)}\right) \quad (1)$$

$$z^{(l+1)} = W^{(l,1)}a^{(1)} + b^{(l+1)} \quad (2)$$

On the other hand, decoding component of each layer uses reverse order functions as given in (3) and (4).

$$a^{(n+l)} = f\left(z^{(n+l)}\right) \quad (3)$$

$$z^{(n+l+1)} = \mathrm{W}^{(\mathrm{n}-l,2)}\mathrm{a}^{(\mathrm{n}+l)} + \mathrm{b}^{(\mathrm{n}-l+2)} \quad (4)$$

In our proposed model, we extract high order features from the vector presentation of the input fundus images, where the extracted features and allied information are accumulated within$a^{(n)}$. This extracted feature is later used to perform classification by mapping it as feature vector for SVM classifier. Noticeably, in SAE model we have applied five Convolutional Layers, here onwards indicated as CONV, 3 Max-pooling layer and one Fully Connected layer. The detailed discussion of these layers is given in the sub-sequent sections. In addition to the features extracted by SAE model, w have incorporated transferable CNN, commonly known as AlexNet-CNN to perform high dimensional feature extraction. The detailed discussion of the AlexNet CNN model is given in the sub-sequent sections.

b). AlexNet CNN based High Dimensional Feature Extraction

Though, AlexNet CNN which was proposed mainly for normal or object image classification, it can be transferred to a CNN structures possessing capacity to extract features from the user specified input images. Such efficiency has helped AlexNet to be used for different biomedical data

analysis and classification. One of the noticeably efficiency of AlexNet CNN is that it can extract high dimensional features without imposing computational overheads. High dimensional features often provides more significant information to make more efficient classification, which is must for our intended glaucoma detection and classification system. With this motive, in this paper AlexNet CNN has been applied to extract high dimensional features (here, we have obtained 4096 dimensional features). Our proposed AlexNet CNN model applies five Convolutional layers (i.e., CONV1, CONV2, CONV3, CONV4 and CONV5) and three Fully Connected Layers (FC6, FC7, FC8). Unlike Differential Algorithm (DA) based SAE CNN, in AlexNet CNN we have applied CaffeNet model [76] that helps alleviating the problem of over-fitting during learning. On the other hand, the use of CaffeNet helps avoiding the need of Graphical Processing Unit (GPU) and hence the proposed model can be executed even on Central Processing Unit (CPU) without any sophisticated hardware availability. The graphical presentation of Alex-Net CNN model is given in Fig. 2.

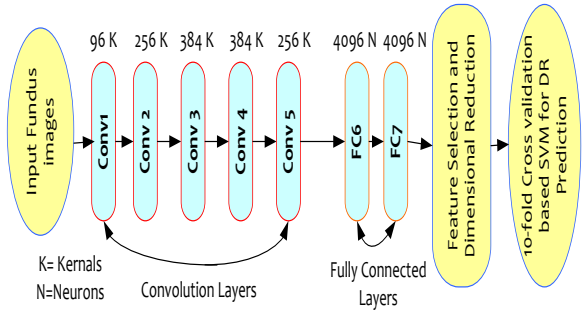

Fig. 2 AlexNet CNN architecture

The detailed discusion of the different layers of AlexNet CNN and fucntional paradigm is given as follows:

- *Input Layer*

In AlexNet-CNN fundus images are fed as input that in later stage generates features as the CONV layers. To achieve better performance we have used a feature scaling and mean subtraction method where the input images which are already processed for resizing are fed as input of CONV layer. In addition, at input layer we define the total number of channels (here, for RGB we used 3).

- *Convolutional Layers*

CONV can be stated as the combination of filters which are capable of extracting certain specific patterns or features from the input image. In our case, CONV extracts the features from the funds images which are obtained as the output and signifies the feature map characterising specific Glaucomatic features. Noticeably, each neuron in the extracted feature map share similar set of weights (W) and bias (b) values that enables neurons in a feature map to detect the similar feature (depicting Glaucomatic traits). Another feature maps in CONV employ different sets of biases and weights to enable extraction of the different local features. In our proposed AlexNet-CNN model, CONV layer filters the input fundus images to retrieve a single feature map as output. As already stated, our proposed AlexNet CNN model comprises five CONV layers; CONV1, CONV2, CONV3, CONV4 and CONV5 where the kernel size is considered as 5×5 with zero-padding performed at 2. In our proposed AlexNet CNN model the convolution layer stride is fixed at 3. Noticeably, the kernel specification at CONV layer is CONV1-96 kernels, CONV2-256 kernels, CONV3-384 kernels, CONV4-384 kernels and CONV5-256 kernels.

- *Max-Pooling Layers*

In GlaucoNet model, pooling layer functions as feature selection layers where it sequentially minimizes the spatial resolution of the individual feature map. Additionally, it reduces the number of parameters and computation required by applying local averaging and a sub-sampling technique that significantly helps avoiding the problem of over-fitting. In our proposed AlexNet model we have applied Max-pooling as native structure of CNN so as to obtain translation-invariant representations in the input fundus images. In our proposed method Max-pooling down-samples the latent representation using a constant component by considering the maximum value over non-overlapping sub-region. Here, Max-pooling considers sparsity over the hidden representation by removing all non-maximal values in non overlapping sub-space and thus it enhances feature detectors to avoid insignificant solutions to carry forward. Similarly, during reconstruction, the derived sparse latent code minimizes the number of filters to decode each pixel and thus makes it more suitable for our intended Glaucoma detection from complex fundus images. Functionally, in our proposed AlexNet CNN model we have applied one Max-pooling layer after each CONV layer, where each layer is defined for 3×3 receptive field with a stride of 3. Here, the receptive filed signifies spatial extent which is achieved by means of classical Max-operation for the defined spatial extent.

- *ReLu Layers*

In addition to the Convolutional Layer, we have considered an additional layer named ReLu that predominantly functions as an activation function. ReLu layer possesses a non linear element-wise operator that functions as a layer. In our proposed AlexNet CNN model we embodied three ReLu layers. With input y, ReLu obtains the output for the neuron $q(y)$ as y if $y > 0$ and $(\delta \times y)$ if $y <= 0$. Here, δ signifies whether we the negative component are required to be ignored by means of multiplication with a slope (Ex. 0.01…) or fixing it to 0. Though, in our proposed model we had assigned $\delta = 0$ that makes it to function similar to the native ReLu function $q(y) = \max(0, y)$. Here, activation is done at zero threshold value.

- *Fully Connected (FC) Layers*

Typically, FC layers functions at the end of the CNN architecture where it performs high-level reasoning tasks. It is also called as classifier layer. FC layers receive a set of neurons (i.e., feature vector) from the preceding layer and maps it to all connected neurons and eventually generates a one-dimensional (feature) vector. It supports CNN to

perform image analysis and classification easily. In our proposed method, AlexNet CNN comprises FC layers that take input data as a simple vector and outputs a single vector. As already stated, in our proposed model we have considered three FC layers; FC6, FC7 and FC8 possessing kernels of 4096, 4096 and 1000 respectively. Considering high dimensional feature requirements, in our proposed method we have considered only FC6 and FC7 with 4096 dimensional features. These obtained features are projected as a feature vector which is concatenated with the features extracted by means of SAE. Considering large scale features extracted that eventually could make classification time consuming and even overburdened. In addition, gigantically large feature set can impose unwanted local minima and convergence during training and classification. In such cases, reducing features or the dimensions of the feature vector can help achieving computationally efficient and accurate glaucoma detection and classification. With this motive, in this paper we have applied two popular dimensional reduction methods; Principle Component Analysis (PCA), and Linear Discriminant Analysis (LDA). Noticeably, we have applied these algorithms as standalone dimensional reduction approach that provides comparative outcome towards identification of a novel and robust solution. A snippet of these algorithms (i.e., PCA and LDA) is given as follows:

D) PCA/LDA based Feature Selection and Dimensional Reduction

Undeniably, our proposed GlaucoNet model with hybrid feature extraction (SAE CNN and AlexNet CNN features) obtained deep features; however at the cost of increased feature size that can make overall further learning and classification overburdened. Additionally, it can force learning method to undergo local minima and convergence issue. To avoid such limitations we have applied feature selection and/or dimensional reduction methods that retain only significant features to process further classification. To achieve it, we have applied two well known algorithms PCA and LDA distinctly. A snippet of these feature selection algorithms is given as follows:

a). Principle Component Analysis (PCA)

It is used to find out the feature space from a space of high dimension to low dimension keeping in mind that the obtained feature consists of all the important details. The PCA helps in rotating the image through a p-dimensional feature space axes to a new position called as principle axis. The principle axis 1 has the highest variance followed by axis 2. As a result it is noted that among the extracted images of glaucoma detection all the images can be inter-related to each other. These co-related features are known as Homogeneous features which are considered to be the most expressive features. The PCA helps in transferring the feature attributes which are homogenous in nature from of one vector to another vector having no co-relation elements. Hence by applying the PCA method a huge number of unwanted feature elements can be reduced which will help in easy and efficient computation. The resultant feature vector obtained makes the computation more efficient. The final resultant vector is then used for classification.

b). Linear Discriminant Analysis (LDA)

Linear Discriminant Analysis (LDA) makes use of the most discriminating features (MDF) for dimensionality reduction. Whereas the PCA which uses the MEF for dimensionality reduction of the data. The LDA is used to perform dimensionality reduction automatically. The LDA is used to project the final resultant features obtained on to a single principle component irrespective of its class labels during the execution process of PCA. For the process of feature extraction and dimensionality reduction the LDA makes use of two different matrix one is the intra-class scatter matrix D_{ISW} and the second one is inter-class scatter matrix D_{IOS}. These matrix values are estimated as follows:

$$D_{ISW} = \sum_{i=1}^{T} \sum_{j=1}^{S_{ci}} (y_j - v_{ci})(y_j - v_{ci})^T \quad (5)$$

$$D_{IOS} = \sum_{i=1}^{T} (v_{ci} - v_c)(v_{ci} - v_c)^T, \quad (6)$$

In (6) T refers the total number of classes, v_{ci} signifies average vector of class i, and S_{ci} presents the overall samples in class i. We estimate v_{ci} as:

$$v_c = \frac{1}{T} \sum_{i=1}^{T} v_{ci}, \quad (7)$$

In (7) T refers the total number of classes. LDA intends to increase the inter-class scatter and decrease the intra-class scatter. In our model, it was achieved by increasing $\mathcal{F}_i$, given in (8).

$$\mathcal{F}_i = \frac{\Delta|S_B|}{\Delta|S_w|} \quad (8)$$

For a non-singular D_{IOS}, F_i is increased provided the column vectors of the projection matrix P are the eigenvectors of $D_{ISW}{}^{-1}D_{IOS}$. Here, the projection matrix P with $T-1$ dimension projects the training data to form Fisher vector (FV). In this way, the final Fischer Vector obtained is given as input to the classifier. Noticeably, the overall Fischer Vectors projected for classification be

$\mathcal{F}_{VC} = (\mathcal{F}_{1C}, \mathcal{F}_{2C}, \mathcal{F}_{3C}, \dots, \mathcal{F}_{4096C})$.

Once the final resultant feature vector is obtained it is further processed for glaucoma classification. The proposed system works on a two class classification which will be classified as Glaucomatic and non Glaucomatic. To improve the performance 10-fold cross validation is performed. A brief description of the classification technique is given as follows:

d. Two-class classification using SVM with N-Fold Cross validation

Major AE based feature extraction and classification systems apply native CNN structure with Convolutional layers, Maxpool and Fully Connected layers. During classification, these methods use softmax classifier. On contrary in this paper we have used SVM with 10-fold cross validation for classification. Here, SVM has been applied to train the extracted vectors that are used to obtain maximum margin by obtaining low m as given in (9).

$$\frac{1}{2}m^T m + e_r \sum E_i, \quad (9)$$

where, $E_i \geq 0$ and e_r signify the extent of error resiliency.

To perform two-class classification, retrieved features from SAE and AlexNet CNN are concatenated together to form a feature vector, which is grouped in the labeled pairs, say K_i (s_i, t_i) where s_i presents the training vector. The class label of the training vector s_i is given by $t_i \in \{-1, 1\}$. In classification the hyper plane classifies the maximum possible points of the same class on the same side of hyperplane. The use of 10-fold cross-validation ensures higher accuracy and reliability of the results. The overall performance of the proposed GalucoNet+ model is examined in terms of classification accuracy and the obtained results are compared with other state-of-art techniques.

VI. RESULTS AND DISCUSSION

Considering the significance of high dimensional deep or fine grained features for glaucoma detection and classification, in this paper the focus was made on incorporating multiple advanced deep learning models. Architecturally, the proposed model was designed as a cascaded model in which at first a Stacked Auto-Encoder (SAE) model was deployed to extract low dimensional features, which was followed by (or in parallel) the execution of a transferable CNN model known as AlexNet CNN. Thus, implementing these two CNN architectures over two well known datasets, DRISHTI-GS and DRION-DB two distinct feature sets were obtained. Recalling structure of SAE model we considered native encoder and decoder paths, where each encoder exhibited CONV with a distinct filter bank to generate a set of encoder feature maps. Towards this objective, we used element-wise rectified-linear non-linearity (ReLU) activation function. On the other hand, at decoder we used CONV layer to generate the decoder feature map. Here, the skip connections transfer the subsequent feature map from encoder path and concatenate it to up-sampled decoder feature maps. In our implemented SAE model we retained 3 CONV, and one FC layer to keep low computational overheads. Once obtaining the extracted feature at FC layer, it was concatenated with the features obtained using AlexNet CNN. Noticeably, to implement CNN unlike conventional ImageNet pre-trained features, we applied our own input data which was processed for feature extraction using CaffeNet. The overall AlexNet-CaffeNet based CNN structure was simulated with VLFeat tool [77]. Unlike SAE model developed as the first layer of feature extraction, we designed AlexNet CNN with five CONV, followed by 3 FC layers, where FC6 and FC7 extracted 4096 dimensional features to process further. In both CNN models, we used training rate gamma as 0.0001, while the drop-rate was fixed at 0.5 (50%) that helped retaining only significant features for further classification. Obtaining the extracted features from SAE and AlexNet CNN we concatenated both to project a feature map to be further processed for dimensional reduction using PCA and LDA. Noticeably, these feature selection methods were applied in distinctly. In PCA implementation the correlation coefficient was selected as 0.5 that retained only 50% significant or superior features by dropping less significant 50% feature attributes. This method was applied primarily to retain significant features by dropping insignificance one, which eventually accomplished computationally efficient CAD model. Unlike conventional deep learning methods where classical entropy gain parameters are used to perform classification, in this paper we used SVM classifier with different kernel functions such as Linear, Polynomial and Radial Basis Function (RBF). In addition, to achieve higher accuracy we used 10-fold cross validation that avoided any predefined or manually defined training and testing data. This approach enabled achieving higher accuracy without imposing additional computational overheads. The overall proposed model was developed on MATLAB 2018a software tool, while the simulation was made on Microsoft Windows 2010 with 8 GB RAM and I5 processor.

To examine performance efficiency of the proposed glaucoma detection and classification system different performance matrix such as true positive (TP), true negative (TN), false positive (FP) and false negative (FN) have been obtained. Further, these matrix values have been used to obtain Accuracy, Precision, F-Measure, and Recall. The mathematical equation and the definition of the derived confusion matrix variables are given in Table II. The performance parameters and their respective values are given in Table III.

Table II Performance Parameters or Criteria

Parameter	Mathematical Expression
Accuracy	$\frac{(TN+TP)}{(TN+FN+FP+TP)}$
Precision	$\frac{TP}{(TP+FP)}$
F-measure	$2.\frac{Recall.Precision}{Recall+Precision}$
Recall or Sensitivity	$\frac{TP}{(TP+FN)}$

Table III Performance comparison with different SVM Kernel functions

Parameter	DRISHTI-GS			DRION-DB		
	SVM-LIN (%)	SVM-POLY (%)	SVM-RBF (%)	SVM-LIN (%)	SVM-POLY (%)	SVM-RBF (%)
Accuracy	92.6	98.8	97.5	90.4	97.5	95.4
Precision	91.9	97.5	96.4	92.0	95.5	96.5
Recall	92.0	97.5	96.4	92.7	95.0	95.5
F-Measure	90.8	97.8	95.5	91.5	95.5	97.5

Observing above results, it can be found that the proposed GlaucoNet+ model exhibits better in conjunction with the

polynomial kernel based SVM classifier. Results affirm that the proposed glaucoma detection and classification system exhibits the maximum accuracy of 98.8% for DRISHTI-GS dataset and 97.5% for DRION-DB dataset. Similarly, the precision of 97.5% and 95.5% for DRISHTI-GS and DRION-DB datasets, respectively affirms robustness and consistency of the proposed glaucoma detection and classification model. Recall, which characterizes sensitiveness of the model too is 97.5% for DRISHTI dataset (while 95.0% for DRION-DB), which applauds its efficacy. Noticeably, the proposed model for the different datasets had very less variation in sensitiveness (2.5%) that shows its reliability in performance. The maximum F-Measure obtained for the proposed GlaucoNet+ model is 97.8%, which is higher than major existing state-of-art techniques. Exploring in depth, it can be found that the polynomial kernel function enables SVM to learn patterns over broad scale or range that makes better hyper-plane identification and hence makes classification better. On contrary, linear kernel function do lack over learning varying features or non-linear features which can be common for the glaucoma traits or features. It can be the prime reason behind the superior performance by SVM with polynomial kernel function than that with the linear kernel function. Though, RBF algorithm makes SVM performing better, especially for non-linear features or patterns, in our proposed model, it could not exhibit better than SVM with polynomial kernel function; though the performance for the both SVM with polynomial and SVM with RBF are close. Summarily, the results affirm that the proposed GlaucoNet+ model can provide the best performance with polynomial kernel based SVM. To further examine the performance of the proposed GlaucoNet+ model which comprises two parallel feature extraction techniques; SAE and AlexNet CNN, we have obtained performance by each approach, which has been further compared with each other. Table IV presents the intra-model comparison of the SAE, AlexNet CNN and proposed (hybrid model with SAE and AlexNet CNN) feature extraction method.

Table IV Intra-model comparison

Parameter	DRISHTI-GS			DRION-DB		
	SAE-CNN (%)	AlexNet-CNN (%)	Hybrid (Proposed) (%)	SAE-CNN (%)	AlexNet-CNN (%)	Hybrid (Proposed) (%)
Accuracy	98.2	97.5	98.8	96.3	92.7	97.5
Precision	94.6	95.5	97.5	93.9	95.5	95.5
Recall	99.0	95.5	97.5	94.2	94.1	95.0
F-Measure	94.1	94.4	97.8	94.1	94.0	95.5

As depicted in Table IV, it can be found the accuracy of the proposed Hybrid CNN model for DRISHTI-GS datasets (noticeably, we have implemented both SAE CNN and AlexNet CNN in parallel, whose features have been fused together using concatenation method) outperforms SAE CNN and AlexNet CNN individually. Here, our proposed method has exhibited accuracy of 98.8% for glaucoma detection and classification, while SAE CNN and AlexNet CNN could achieve relative accuracy of 98.2% and 97.5%, respectively. Similarly, our proposed approach achieved accuracy of 97.5% which is higher than SAE CNN (94.6%) as well as AlexNet CNN (95.5%). The similar performance can be observed for recall as well as F-Measure (Table IV). Considering, glaucoma detection and classification efficacy of the proposed GlaucoNet+ model it can be found that the proposed hybrid feature extraction based model outperforms other approaches. It signifies that the use of deep features can achieve higher accuracy and performance reliability. Table V presents the comparison of the performance by GlaucoNet+ model with PCA and LDA based selected features. Observing the results, it can be found that the proposed model with LDA feature selection can achieve higher performance than PCA based selected features.

Table V Performance assessment with different feature selection methods with DRISHTI-GS dataset

Parameter	GlaucoNet+ PCA	GlaucoNet+ LDA
Accuracy	94.2	98.8
Precision	95.5	97.5
Recall	95.5	97.5
F-Measure	91.0	97.8

Here, LDA which unlike conventional PCA (with 0.5 of the correlation coefficient or significance level) selects significant MDF features. It enables retaining most significant features having better ROI characterizing ability. The efficacy of LDA based method enables GlaucoNet+ to outperform PCA based features. Table III and Table IV discussed performance of the proposed GlaucoNet+ model with different classification setups (Table III) and configuration (Table IV); however to further examine efficacy of our proposed model in comparison to the other existing glaucoma detection and classification methods, we have performed analysis based on secondary resources (reviewing existing methods or allied papers). Table VI presents the comparative performance by the proposed model.

Table VI Comparative Performance Analysis

Reference	Accuracy (%)	Precision (%)	Recall (%)	F-Measure (%)
[44]	97.50	-	-	-
[49]	84.38	-	-	-
[54]	95.50	-	-	-
[60]		-	-	-
[64]	88.00	-	-	-
[35]	-	-	98.60	-
[36]	99.20	-	86.00	-
[65]	-	-	-	-
[47]	80.00	-	95.00	-
[48]	97.00	-	-	-
[57]	98	-	-	-
[39]	94.10	-	91.80	-
[75]	90.00	-	-	-
[40]	-	-	92.00	-
[33]	100.00	-	94.00	-
[59]	-	-	-	-
[66]	89.6 (NB) 97.6(ANN)	-	-	-
[67]	92.00	-	-	-
[68]	-	-	-	-
[69]	72.38	-	-	-
[70]	79.00	-	87.00	-
[71]	83.10	-	-	-
[62]	93.00	-	-	-
[72]	96.67	-	100.00	-
[73]	91.00	-	-	-
[74]	92.00	-	-	-
[4]			0.8478	-
[55]	88.7	-	60.6	-
[34]	84.0	-	-	-
GlaucoNet + DRISHTI-GS	98.8	97.5	97.5	97.8
GlaucoNet + DRION-DB	97.5	95.5	95.0	95.5

Observing the results, it can be found that the proposed GlaucoNet+ model with Hybrid feature extraction and SVM (polynomial) with 10-fold cross validation outperforms major existing approaches. The overall results and allied significances affirm robustness of the proposed system over conventional glaucoma detection and classification systems.

The overall research and allied outcomes affirm that the use of hybrid feature extraction method with SAE and AlexNet CNN, which is sometime stated as transferable CNN can be a potential solution to perform glaucoma detection and classification. It affirms the RQ1 as stated in section III. The results obtained in Table III reveal that the SAE with AlexNet CNN can be potential approach to extract or achieve deep features so as to make optimal classification decision. It affirms affirmative answer for RQ2 in Section III. The above results affirms that the proposed GlaucoNet+ model which employs deep features extracted from SAE and AlexNet CNN performs better as compared to SAE and AlexNet CNN individually. It signifies that the use of high dimensional deep features can be more efficient to achieve higher accuracy and classification reliability. It affirms positively towards the RQ3. As depicted in Table IV, it is observed that LDA features which comprises MDF constructs enable achieving higher accuracy than the PCA features. It supports RQ4 affirmatively. As discussed in above discussion, it can be found that the proposed method with SVM (polynomial kernel) in conjunction with N-fold cross validation exhibits superior performance and hence RQ5 defined in Section III is accepted positively. The overall research conclusion for the presented research is given in the sub-sequent section.

VII. CONCLUSION

Considering the significance of high dimensional deep features for image classification model to be used for glaucoma detection in this paper the focus was made on exploiting SAE and a well known transferable CNN structure called AlexNet CNN. This paper proposed a model named GlaucoNet+ which at first used SAE and AlexNet CNN to extract features from the fundus images, which were later fused by feature concatenation. Obtaining the deep features, to maintain optimal balance between computational efficiency and reliability two well known feature selection methods named PCA and LDA were used independently, which as a result enables retaining optimal feature sets for further classification. The selected features were processed for SVM classification with different kernel functions where the uses of N-fold cross validation avoided manual training and testing set selection. This method achieved higher accuracy even at reduced computational overhead. The overall result revealed that the proposed GlaucoNet+ method with hybrid features containing SAE and AlexNet CNN features performs better with LDA based feature selection and SVM with polynomial kernel function. The overall efficacy of the proposed method affirms robustness even with different fundus image datasets having different spatio-temporal features and hence can be applied for real-time CAD solutions for Glaucoma detection and classification.

VIII. ACKNOWLEDGEMENT

We gratefully thank the Visvesvaraya Technological University, Jnanasangama, Belagavi for financial support extended to this research work. Sincere Thanks to my supervisor for providing constant and concurrent support for utilization of computational facilities by FIST grant of DST, VBIT, Ghatkesar, T.S., India, during the progress of this work

REFERENCES

1. Y.-C. Tham, X. Li, T. Y. Wong, H. A. Quigley, T. Aung, and C.-Y. Cheng, "Global prevalence of glaucoma and projections of glaucoma burden through 2040: A systematic review and meta-analysis," Ophthalmology, vol. 121, no. 11, pp. 2081–2090, 2014.
2. S. Y. Shen, T. Y. Wong, P. J. Foster, J.-L. Loo, M. Rosman, S.-C. Loon, W. L. Wong, S.-M. Saw, and T. Aung, "The prevalence and types of glaucoma in malay people: The singaporemalay eye study," Investigative Ophthalmology and Visual Science, vol. 49, no. 9, p. 3846, 2008.
3. Pederson JE and Anderson DR, "The mode of progressive disc cupping in ocular hypertension and glaucoma," Archives of Ophthalmology, vol. 98, no. 3, pp. 490–495, 1980.
4. H. Fu et al., "Disc-Aware Ensemble Network for Glaucoma Screening From Fundus Image," in IEEE Transactions on Medical Imaging, vol. 37, no. 11, pp. 2493-2501, Nov. 2018.
5. J. Jonas, W. Budde, and S. Panda-Jonas, "Ophthalmoscopic evaluation of the optic nerve head," Survey of Ophthalmology, vol. 43, no. 4, pp. 293–320, 1999.
6. J. E. Morgan, N. J. L. Sheen, R. V. North, Y. Choong, and E. Ansari, "Digital imaging of the optic nerve head: monoscopic and stereoscopic analysis," British Journal of Ophthalmology, vol. 89, no. 7, pp. 879–884, 2005.
7. H. Fu, Y. Xu, S. Lin, X. Zhang, D. Wong, J. Liu, and A. Frangi, "Segmentation and Quantification for Angle-Closure Glaucoma Assessment in Anterior Segment OCT," IEEE Trans. Med. Imag., vol. 36, no. 9, pp. 1930–1938, 2017.
8. J. B. Jonas, A. Bergua, P. SchmitzValckenberg, K. I. Papastathopoulos, and W. M. Budde, "Ranking of optic disc variables for detection of glaucomatous optic nerve damage," Invest. Ophthalmol. Vis. Sci., vol. 41, no. 7, pp. 1764–1773, 2000.
9. M. D. HancoxO.D., "Optic disc size, an important consideration in the glaucoma evaluation," Clinical Eye and Vision Care, vol. 11, no. 2, pp. 59 – 62, 1999.
10. G. D. Joshi, J. Sivaswamy, and S. R. Krishnadas, "Optic Disk and Cup Segmentation from Monocular Colour Retinal Images for Glaucoma Assessment," IEEE Trans. Med. Imag., vol. 30, no. 6, pp. 1192–1205, 2011.
11. F. Yin, J. Liu, S. H. Ong, Y. Sun, D. W. K. Wong, N. M. Tan, C. Cheung, M. Baskaran, T. Aung, and T. Y. Wong, "Model-based optic nerve head segmentation on retinal fundus images," in Proc. EMBC, 2011, pp. 2626–2629.
12. J. Cheng, J. Liu, Y. Xu, F. Yin, D. Wong, N. Tan, D. Tao, C.-Y. Cheng, T. Aung, and T. Wong, "Superpixel classification based optic disc and optic cup segmentation for glaucoma screening," IEEE Trans. Med. Imag., vol. 32, no. 6, pp. 1019–1032, 2013.
13. J. Cheng, D. Tao, D. W. K. Wong, and J. Liu, "Quadratic divergence regularized SVM for optic disc segmentation," Biomed. Opt. Express, vol. 8, no. 5, pp. 2687–2696, 2017.
14. H. Fu, J. Cheng, Y. Xu, D. Wong, J. Liu, and X. Cao, "Joint Optic Disc and Cup Segmentation Based on Multi-label Deep Network and Polar Transformation," IEEE Trans. Med. Imag., 2018.
15. J. Cheng, F. Yin, D. W. K. Wong, D. Tao, and J. Liu, "Sparse dissimilarity-constrained coding for glaucoma screening," vol. 62, no. 5, pp. 1395–1403, 2015.
16. R. Bock, J. Meier, L. G. Nyul, J. Hornegger, and G. Michelson, "Glaucoma risk index: Automated glaucoma detection from color fundus images," Medical Image Analysis, vol. 14, no. 3, pp. 471–481, 2010.
17. S. Dua, U. RajendraAcharya, P. Chowriappa, and S. VinithaSree, "Wavelet-based energy features for glaucomatous image classification," IEEE Transactions on Information Technology in Biomedicine, vol. 16, no. 1, pp. 80–87, 2012.
18. K. P. Noronha, U. R. Acharya, K. P. Nayak, R. J. Martis, and S. V. Bhandary, "Automated classification of glaucoma stages using higher order cumulant features," Biomedical Signal Processing and Control, vol. 10, no. 1, pp. 174–183, 2014.
19. U. R. Acharya, E. Ng, W. Eugene, Lim, K. Noronha, L. Min, K. Nayak, and S. Bhandary, "Decision support system for the glaucoma using Gabor transformation," Biomedical Signal Processing and Control, vol. 15, pp. 18–26, 2015.
20. A. Krizhevsky, I. Sutskever, and G. Hinton, "Imagenet classification with deep convolutional neural networks," in Proc. NIPS, 2012, pp. 1097–1105.
21. V. Gulshan, L. Peng, M. Coram, and et.al, "Development and Validation of a Deep Learning Algorithm for Detection of Diabetic Retinopathy in Retinal Fundus Photographs," Journal of the American Medical Association, vol. 304, no. 6, pp. 649–656, 2016.
22. A. Esteva, B. Kuprel, R. A. Novoa, J. Ko, S. M. Swetter, H. M. Blau, and S. Thrun, "Dermatologist-level classification of skin cancer with deep neural networks," Nature, vol. 542, no. 7639, pp. 115–118, 2017.
23. D. Shu Wei Ting and et al., "Development and Validation of a Deep Learning System for Diabetic Retinopathy and Related Eye Diseases Using Retinal Images From Multiethnic Populations With Diabetes," JAMA, vol. 318, no. 22, pp. 2211–2223, 2017.
24. Q. Li, B. Feng, L. Xie, P. Liang, H. Zhang, and T. Wang, "A Cross modality Learning Approach for Vessel Segmentation in Retinal Images," IEEE Trans. Med. Imag., vol. 35, no. 1, pp. 109–118, 2016.
25. H. Fu, Y. Xu, S. Lin, D. W. K. Wong, and J. Liu, "DeepVessel: Retinal Vessel Segmentation via Deep Learning and Conditional Random Field," in Proc. MICCAI, 2016, pp. 132–139.
26. X. Chen, Y. Xu, S. Yan, D. Wing, T. Wong, and J. Liu, "Automatic Feature Learning for Glaucoma Detection Based on Deep Learning," in Proc. MICCAI, 2015, pp. 669–677.
27. J. I. Orlando, E. Prokofyeva, M. Del Fresno, and M. B. Blaschko, "Convolutional neural network transfer for automated glaucoma identification," in Proc. SPIE, 12th International Symposium on Medical Information Processing and Analysis, 2016.
28. S. Yousefi et al., "Learning From Data: Recognizing Glaucomatous Defect Patterns and Detecting Progression From Visual Field Measurements," in IEEE Trans. on Biomedical Engg., vol. 61, no. 7, pp. 2112-2124, July 2014.
29. R. Panda, N. B. Puhan, A. Rao, D. Padhy and G. Panda, "Recurrent neural network based retinal nerve fiber layer defect detection in early glaucoma," 2017 IEEE 14th International Symposium on Biomedical Imaging (ISBI 2017), Melbourne, VIC, 2017, pp. 692-695.
30. M. E. Şahin and M. R. Bozkurt, "Retinal Nerve Fiber Layer detection at Optical Coherence Tomography image for the diagnosis of glaucoma," 2015 Medical Technologies National Conference, Bodrum, 2015, pp. 1-3.
31. Aslan, Muhammet&Ceylan, Murat &Durdu, Akif. (2018). Segmentation of Retinal Blood Vessel Using Gabor Filter and Extreme Learning Machines. 10.1109/IDAP.2018.8620890.

32. A. Gopalakrishnan, A. Almazroa, K. Raahemifar and V. Lakshminarayanan, "Optic disc segmentation using circular hough transform and curve fitting," 2015 2nd International Conference on Opto-Electronics and Applied Optics, Vancouver, BC, 2015, pp. 1-4.
33. T. Khalil, M. UsmanAkram, S. Khalid and A. Jameel, "Improved automated detection of glaucoma from fundus image using hybrid structural and textural features," in IET Image Proc., vol. 11, no. 9, pp. 693-700, 9 2017.
34. N. Kavya and K. V. Padmaja, "Glaucoma detection using texture features extraction," 2017 51st Asilomar Conference on Signals, Systems, and Computers, Pacific Grove, CA, 2017, pp. 1471-1475.
35. S. Omid, J. Shanbehzadeh, Z. Ghassabi and S. S. Ostadzadeh, "Optic disc detection in high-resolution retinal fundus images by region growing," 2015 8th International Conference on Biomedical Engineering and Informatics (BMEI), Shenyang, 2015, pp. 101-105.
36. M. Lotankar, K. Noronha and J. Koti, "Detection of optic disc and cup from color retinal images for automated diagnosis of glaucoma," 2015 IEEE UP Section Conference on Electrical Computer and Electronics (UPCON), Allahabad, 2015, pp. 1-6.
37. G. Pavithra, A. Tugashetti, T. C. Manjunath and L. Dharmanna, "Investigation of primary glaucoma by CDR in fundus images," 2017 2nd IEEE International Conference on Recent Trends in Electronics, Information & Communication Technology (RTEICT), Bangalore, 2017, pp. 1841-1848.
38. W. Luangruangrong, K. Chinnasarn and A. Rodtook, "Polar Space Contour Detection for Automated Optic Cup Segmentation," 2018 10th International Conference on Knowledge and Smart Technology (KST), Chiang Mai, 2018, pp. 164-169.
39. P. Das, S. R. Nirmala and J. P. Medhi, "Detection of glaucoma using Neuroretinal Rim information," 2016 International Conference on Accessibility to Digital World (ICADW), Guwahati, 2016, pp. 181-186.
40. H. Alghmdi, HongyingLilian Tang, M. Hansen, A. O'Shea, L. Al Turk and T. Peto, "Measurement of optical cup-to-disc ratio in fundus images for glaucoma screening," 2015 International Workshop on Computational Intelligence for Multimedia Understanding (IWCIM), Prague, 2015, pp. 1-5.
41. M. Aloudat and M. Faezipour, "Determination for Glaucoma disease based on red area percentage," 2016 IEEE Long Island Systems, Applications and Technology Conference (LISAT), Farmingdale, NY, 2016, pp. 1-5.
42. M. Roslin and S. Sumathi, "Glaucoma screening by the detection of blood vessels and optic cup to disc ratio," 2016 International Conference on Comm. and Signal Processing, Melmaruvathur, 2016, pp. 2210-2215.
43. S. M. Nikam and C. Y. Patil, "Glaucoma detection from fundus images using MATLAB GUI," 2017 3rd International Conference on Advances in Comp. Comm. & Automation (ICACCA) (Fall), Dehradun, 2017, pp. 1-4.
44. H. Ahmad, A. Yamin, A. Shakeel, S. O. Gillani and U. Ansari, "Detection of glaucoma using retinal fundus images," 2014 International Conference on Robotics and Emerging Allied Technologies in Engineering (iCREATE), Islamabad, 2014, pp. 321-324.
45. E. Pinos-Velez, M. Flores-Rivera, W. Ipanque-Alama, D. Herrera-Alvarez, C. Chacon and L. Serpa-Andrade, "Implementation of support tools for the presumptive diagnosis of Glaucoma through identification and processing of medical images of the human eye," 2018 IEEE International Systems Engineering Symposium (ISSE), Rome, 2018, pp. 1-5.
46. Atheesan S. and Yashothara S., "Automatic glaucoma detection by using funduscopic images," 2016 International Conference on Wireless Communications, Signal Processing and Networking (WiSPNET), Chennai, 2016, pp. 813-817.
47. J. K. Virk, M. Singh and M. Singh, "Cup-to-disk ratio (CDR) determination for glaucoma screening," 2015 1st International Conference on Next Generation Computing Technologies, Dehradun, 2015, pp. 504-507.
48. D. D. Patil, R. R. Manza, G. C. Bedke and D. D. Rathod, "Development of primary glaucoma classification technique using optic cup & disc ratio," 2015 International Conference on Pervasive Computing (ICPC), Pune, 2015, pp. 1-5.
49. D. E. Kusumandari, ArisMunandar and G. G. Redhyka, "The comparison of GVF Snake Active Contour method and Ellipse Fit in optic disc detection for glaucoma diagnosis," 2015 International Conference on Automation, Cognitive Science, Optics, Micro Electro-Mechanical System, and Information Technology (ICACOMIT), Bandung, 2015, pp. 123-126.
50. A. M. Jose and A. A. Balakrishnan, "A novel method for glaucoma detection using optic disc and cup segmentation in digital retinal fundus images," 2015 International Conference on Circuits, Power and Computing Technologies [ICCPCT-2015], Nagercoil, 2015, pp. 1-5.
51. E. Deepika and S. Maheswari, "Earlier glaucoma detection using blood vessel segmentation and classification," 2018 2nd International Conference on Inventive Systems and Control (ICISC), Coimbatore, 2018, pp. 484-490.
52. M. K. Dutta, A. K. Mourya, A. Singh, M. Parthasarathi, R. Burget and K. Riha, "Glaucoma detection by segmenting the super pixels from fundus colour retinal images," 2014 International Conf. on Medical Imaging, m-Health and Emerging Comm. Systems, Greater Noida, 2014, pp. 86-90.
53. K. Choudhary and S. Wadhwa, "Glaucoma Detection Using Cross Validation Algorithm," 2014 Fourth International Conference on Advanced Computing & Communication Technologies, Rohtak, 2014, pp. 478-482.
54. L. Xiong, H. Li and Y. Zheng, "Automatic detection of glaucoma in retinal images," 2014 9th IEEE Conference on Industrial Electronics and Applications, Hangzhou, 2014, pp. 1016-1019.
55. Harshvardhan G, Venkateswaran N and Padmapriya N, "Assessment of Glaucoma with ocular thermal images using GLCM techniques and Logistic Regression classifier," 2016 International Conference on Wireless Communications, Signal Processing and Networking (WiSPNET), Chennai, 2016, pp. 1534-1537.
56. S. Pathan, P. Kumar and R. M. Pai, "The Role of Color and Texture Features in Glaucoma Detection," 2018 International Conference on Advances in Computing, Communications and Informatics (ICACCI), Bangalore, 2018, pp. 526-530.
57. S. Simonthomas, N. Thulasi and P. Asharaf, "Automated diagnosis of glaucoma using Haralick texture features," International Conference on Information Communication and Embedded Systems (ICICES2014), Chennai, 2014, pp. 1-6.
58. Fu, Huazhu& Cheng, Jun &Xu, Yanwu& Zhang, Changqing& Wing Kee Wong, Damon & Liu, Jiang & Cao, Xiaochun. (2018). Disc-Aware Ensemble Network

for Glaucoma Screening From Fundus Image. IEEE Transactions on Medical Imaging. PP. 1-1. 10.1109/TMI.2018.2837012.
59. A. Pal, M. R. Moorthy and A. Shahina, "G-Eyenet: A Convolutional Autoencoding Classifier Framework for the Detection of Glaucoma from Retinal Fundus Images," 2018 25th IEEE International Conference on Image Processing (ICIP), Athens, 2018, pp. 2775-2779.
60. X. Chen, Y. Xu, D. W. Kee Wong, T. Y. Wong and J. Liu, "Glaucoma detection based on deep convolutional neural network," 2015 37th Annual International Conference of the IEEE Engineering in Medicine and Biology Society (EMBC), Milan, 2015, pp. 715-718.
61. F. Calimeri, A. Marzullo, C. Stamile and G. Terracina, "Optic Disc Detection Using Fine Tuned Convolutional Neural Networks," 2016 12th International Conference on Signal-Image Technology & Internet-Based Systems (SITIS), Naples, 2016, pp. 69-75.
62. J. Kim, S. Candemir, E. Y. Chew and G. R. Thoma, "Region of Interest Detection in Fundus Images Using Deep Learning and Blood Vessel Information," 2018 IEEE 31st International Symposium on Computer-Based Medical Systems (CBMS), Karlstad, 2018, pp. 357-362.
63. V. Nair and G. E. Hinton. Rectified linear units improve restricted boltzmann machines. In Proc. 27th International Conference on Machine Learning, 2010.
64. A. John, A. Sharma, H. Singh and V. Rehani, "Fuzzy based decision making for detection of Glaucoma," 2017 8th International Conference on Computing, Communication and Networking Technologies (ICCCNT), Delhi, 2017, pp. 1-6.
65. C. Gisler, A. Ridi, M. Fauquex, D. Genoud and J. Hennebert, "Towards glaucoma detection using intraocular pressure monitoring," 2014 6th International Conference of Soft Computing and Pattern Recognition (SoCPaR), Tunis, 2014, pp. 255-260.
66. G. R., P. V. Rao and A. S., "Automated glaucoma detection system based on wavelet energy features and ANN," 2014 International Conference on Advances in Computing, Communications and Informatics (ICACCI), New Delhi, 2014, pp. 2808-2812.
67. J. Ayub et al., "Glaucoma detection through optic disc and cup segmentation using K-mean clustering," 2016 International Conference on Computing, Electronic and Electrical Engg., Quetta, 2016, pp. 143-147.
68. Y. Hatanaka et al., "Improved automated optic cup segmentation based on detection of blood vessel bends in retinal fundus images," 2014 36th Annual International Conference of the IEEE Engineering in Medicine and Biology Society, Chicago, IL, 2014, pp. 126-129.
69. A. Chakravarty and J. Sivaswamy, "Glaucoma classification with a fusion of segmentation and image-based features," 2016 IEEE 13th International Symposium on Biomedical Imaging (ISBI), Prague, 2016, pp. 689-692.
70. A. Ramzan, M. UsmanAkram, A. Shaukat, S. GulKhawaja, U. UllahYasin and W. Haider Butt, "Automated glaucoma detection using retinal layers segmentation and optic cup-to-disc ratio in optical coherence tomography images," in IET Image Processing, vol. 13, no. 3, pp. 409-420, 28 2 2019.
71. A. Agarwal, A. Issac, A. Singh and M. K. Dutta, "Automatic imaging method for optic disc segmentation using morphological techniques and active contour fitting," 2016 Ninth International Conference on Contemporary Computing (IC3), Noida, 2016, pp. 1-5.
72. Harini R and Sheela N, "Feature extraction and classification of retinal images for automated detection of Diabetic Retinopathy," 2016 Second International Conference on Cognitive Computing and Information Processing, Mysore, 2016, pp. 1-4.
73. E. Santos, L. Santos, R. Veras, M. Frazao and D. Leite, "A Semiautomatic Superpixel Based Approach to Cup-to-Disc Ratio Measurement," 2018 IEEE Symposium on Comp. and Comm., Natal, 2018, pp. 00621-00626.
74. S. A. Tuncer, T. Selçuk, M. Parlak and A. Alkan, "Hybrid approach optic disc segmentation for retinal images," 2017 International Artificial Intelligence and Data Processing Symposium, Malatya, 2017, pp. 1-5.
75. A.Agarwal, S. Gulia, S. Chaudhary, M. K. Dutta, C. M. Travieso and J. B. Alonso-Hernández, "A novel approach to detect glaucoma in retinal fundus images using cup-disk and rim-disk ratio," 2015 4th International Work Conference on Bioinspired Intelligence (IWOBI), San Sebastian, 2015, pp. 139-144.
76. Y. Jia, et al., "Caffe: Convolutional architecture for fast feature embedding," in Proceedings of the ACM International Conference on Multimedia. ACM, pp. 675–678, 2014.
77. http://www.vlfeat.org/